



1 **Oxygen Utilization and Downward Carbon Flux in an**  
2 **Oxygen-Depleted Eddy in the Eastern Tropical North**  
3 **Atlantic**

4  
5 **B. Fiedler<sup>1</sup>, D. Grundle<sup>1</sup>, F. Schütte<sup>1</sup>, J. Karstensen<sup>1</sup>, C.R. Löscher<sup>1</sup>, H. Hauss<sup>1</sup>,**  
6 **H. Wagner<sup>1</sup>, A. Loginova<sup>1</sup>, R. Kiko<sup>1</sup>, P. Silva<sup>2</sup>, and A. Körtzinger<sup>1,3</sup>**

7 [1] GEOMAR, Helmholtz Centre for Ocean Research Kiel, Germany

8 [2] Instituto Nacional de Desenvolvimento das Pescas (INDP), Cape Verde

9 [3] Christian Albrecht University Kiel, Germany

10 Correspondence to: B. Fiedler (bfiedler@geomar.de)

11

12 **Abstract**

13 The occurrence of mesoscale eddies that develop an extreme low oxygen environment at  
14 shallow depth (about 40 to 100 m) has recently been reported for the eastern tropical North  
15 Atlantic (ETNA). Their hydrographic structure suggests that the water mass inside the eddy is  
16 well isolated from ambient waters supporting the development of severe near-surface oxygen  
17 deficits. So far, hydrographic and biogeochemical characterization of these eddies was limited  
18 to a few autonomous surveys, using moorings, underwater gliders and profiling floats. In this  
19 study we present results from the first dedicated biogeochemical survey of one of these eddies  
20 conducted in March 2014 near the Cape Verde Ocean Observatory (CVOO). At the time of  
21 the survey the eddy core showed lowest oxygen concentrations of less than 5  $\mu\text{mol kg}^{-1}$  and a  
22 pH of approx. 7.6 at the lower boundary of the euphotic zone. Correspondingly, the aragonite  
23 saturation level dropped to 1 thereby creating unfavorable conditions for calcifying organisms  
24 at this shallow depth. To our knowledge, such enhanced acidity within near-surface waters  
25 has never been reported before for the open Atlantic Ocean. Vertical distributions of  
26 particulate and dissolved organic matter (POM, DOM) generally show elevated  
27 concentrations in the surface mixed layer, but particularly DOM also accumulates beneath the  
28 oxygen minimum. Considering reference data from the upwelling region where these eddies  
29 are formed, we determined the oxygen consumption through remineralization of organic



1 matter and found an enhancement of apparent oxygen utilization rates (aOUR,  $0.26 \mu\text{mol kg}^{-1}$   
2  $\text{d}^{-1}$ ) by almost one order of magnitude when compared with typical values for the open North  
3 Atlantic. Computed downward fluxes for particulate organic carbon (POC) at 100 m were  
4 about  $0.19$  to  $0.23 \text{ g C m}^{-2} \text{ d}^{-1}$  which clearly exceed fluxes typical for an oligotrophic open  
5 ocean setting. The observations support the view that the oxygen depleted eddies can be  
6 viewed as isolated, westwards propagating upwelling systems as their own.

7

## 8 **1 Introduction**

9 New technological advances in ocean observation platforms, such as profiling floats, gliders,  
10 and in sensors have greatly facilitated our knowledge about physical, chemical and biological  
11 processes in the oceans, and particularly those occurring on small spatio-temporal scales  
12 (Johnson et al., 2009; Roemmich et al., 2009). In particular physical transport processes in  
13 frontal regions and in mesoscale eddies have been found to generate biogeochemical  
14 responses that are very different from the general background conditions (Baird et al., 2011;  
15 Mahadevan, 2014; Stramma et al., 2013). A key process in driving the generation of  
16 anomalies is the vertical flux of nutrients into the euphotic zone that enhances primary  
17 productivity, a process that is of particular importance in usually oligotrophic environments  
18 (Falkowski et al., 1991; McGillicuddy et al., 2007). Besides the locally generated response,  
19 the westward propagation of mesoscale eddies introduce a horizontal (mainly zonal)  
20 relocation of eddy properties. Satellite data and model studies show that eddies do play an  
21 important role in the offshore transport of organic matter and nutrients from eastern boundary  
22 upwelling systems (EBUS) into the open ocean. Considering their transport alone, eddies  
23 have been found to create a negative impact on productivity in EBUS regions because of their  
24 net nutrient export (Gruber et al., 2011; Nagai et al., 2015; Rossi et al., 2009).

25 The eastern tropical North Atlantic (ETNA) hosts an eastern boundary oxygen minimum zone  
26 (OMZ) which is primarily created from sluggish ventilation (Luyten et al., 1983) and high  
27 productivity in the EBUS along the West African coast. In its western part, the ETNA is  
28 bounded by the Cape Verde frontal zone (CVFZ) separating the OMZ regime from the wind  
29 driven and well ventilated North Atlantic subtropical gyre. In the south, towards the equator,  
30 oxygen is supplied via zonal current bands (Stramma et al., 2005; Brandt et al. 2015). The  
31 vertical oxygen distribution shows two distinct oxygen minima, an upper one at about 75m  
32 depth and a deep OMZ core at about 400 m (Brandt et al., 2015; Karstensen et al., 2008;



1 Stramma et al., 2008b). On the large scale, the minimum oxygen concentrations in the ETNA  
2 OMZ are just below  $40 \mu\text{mol kg}^{-1}$  (Stramma et al., 2009) but an expansion of the OMZ both  
3 in terms of intensity and vertical extent has been observed over periods of decades (Stramma  
4 et al., 2008a). However, recently Karstensen et al. (2015) reported the appearance of very low  
5 oxygen concentrations at very shallow depth, close to the mixed layer base, in the ETNA in a  
6 long term oxygen time series from a mooring at the Cape Verde Ocean Observatory (CVOO,  
7 [cvo0.geomar.de](http://cvo0.geomar.de)) and from a profiling float. By making use of satellite derived sea level  
8 anomaly data, the authors could associate the occurrence of the low oxygen events with  
9 cyclonic (CE) as well as anticyclone mode-water eddies (ACMEs). Normal anticyclones did  
10 not show any low oxygen signature. They also propose that the oxygen minimum in CEs and  
11 ACMEs is not being exported from the eddy formation region (along the west African coast)  
12 but created during the westward passage of the eddies into the open ETNA.

13 Based on satellite data analysis a statistical assessment of mesoscale eddies has been done for  
14 the North Atlantic in general (Chelton et al., 2011) as well as for the ETNA in particular  
15 (Chaigneau et al., 2009; Schütte et al., 2015). However, Schütte et al. (2015 & in prep. for this  
16 issue) were the first to further differentiate anticyclonically rotating eddies into “normal”  
17 anticyclones and ACMEs by combining satellite data (sea level anomalies, sea surface  
18 temperature) with in-situ data (CTD, profiling floats, glider). They found that about 1 to 2  
19 ACMEs are generated each year (at distinct regions in the EBUS) that propagate into the open  
20 ETNA waters.

21 An intense biogeochemical response in ACMEs has been reported for other ocean regions as  
22 well. For instance, McGillicuddy et al. (2007) reported intense phytoplankton blooms in  
23 ACMEs for the western North Atlantic, near Bermuda. They explained the phenomenon as  
24 the result of a vertical nutrient flux driven by the interaction of the eddy with the overlying  
25 wind field. Altabet et al. (2012) observed enhanced production of biogenic nitrogen ( $\text{N}_2$ )  
26 inside an ACME in the generally suboxic conditions in the eastern South Pacific OMZ.  
27 Further, consequences for carbon cycling such as production and export, as well as the impact  
28 on the ETNA OMZ also remain unclear.

29 However, detailed process understanding of the physical and biogeochemical processes and  
30 their linkages in eddies, in particular in the high productive ACMEs, is still scarce and one  
31 reason is the difficulty in performing dedicated in-situ surveys of such eddies. Here, we  
32 present the first biogeochemical insights into low-oxygen ACMEs in the ETNA based on



1 direct in situ sampling during two coordinated ship-based surveys. This publication is part of  
2 a series that describe biological, chemical and physical oceanographic processes in low-  
3 oxygen ACMEs in the ETNA. In this paper we first present the vertical hydrographic  
4 structure of a surveyed ACME and discuss nutrients concentrations and the marine carbonate  
5 system. All data are put into regional context by comparing ACME conditions with 1)  
6 ambient background conditions represented by the nearby Cape Verde Ocean Observatory  
7 time-series site (CVOO) and 2) the biogeochemical setting in the proximal EBUS off the  
8 West African coast, where the eddy originated from. We then provide estimates for  
9 transformation rates of various key parameters and derive estimates for carbon export rates  
10 within the surveyed ACME in the ETNA.

11

## 12 **2 Methods**

13 Mesoscale eddies can be detected and tracked from space (Chelton et al., 2011; Schütte et al.,  
14 2015). However, only a few of such eddies develop an oxygen depleted core and a targeted  
15 survey of oxygen-depleted mesoscale eddies in the ETNA (and elsewhere) is challenging.  
16 (Schütte et al., in prep. for this issue) analysed satellite and corresponding in-situ data and  
17 found that on average about 20% of all anticyclones (10% of all eddies) are ACMEs in the  
18 ETNA exhibit a strong low oxygen core. CEs also develop a low oxygen core but not as low  
19 as ACMEs do.

20 In order to enable a targeted survey of the one particular ACME the following strategy was  
21 designed (“Eddy Hunt” project; Körtzinger et al., introduction to this special issue): we  
22 combined satellite data (sea level anomaly, SLA, and sea surface temperature, SST) with  
23 Argo float data in a near-real time mode. Although we did not had access to oxygen data in  
24 near-real time we knew from earlier observations (Karstensen et al., 2015) that low oxygen  
25 ACMEs have a low salinity core. As such, detecting an eddy with high SLA and low SST  
26 (note, normal anticyclones show high SST; Schütte et al., 2015) and confirming low salinity  
27 at shallow depth from opportunistic Argo float data, potential low-oxygen ACMEs were  
28 detected. A pre-survey (with an autonomous underwater glider) of one such candidate ACME  
29 confirmed a low oxygen core and ship surveys were initiated.

30 Here, we use ship data as well as data from a profiling float of a variety of biogeochemical  
31 parameters in order to investigate the marine carbonate system functioning on low-oxygen  
32 eddies. The following sections will provide a brief overview of samples collected during two



1 ship cruises and the applied analytical methods. Moreover, the general setting of the CVOO  
2 ship time series as well as data from hydrographic cruises and the profiling float will be  
3 introduced.

## 4 **2.1 Eddy Surveys**

5 Dedicated eddy surveys were done during the RV Islandia cruise ISL\_00314 (05 March – 07  
6 March 2014; hereafter named ISL) and the RV Meteor cruise M105 (17 March to 18 March  
7 2014; hereafter named M105). During both cruises hydrographic and biogeochemical data  
8 was sampled in the same eddy (Figure 1). Water samples were collected with a rosette water  
9 sampling system equipped with a CTD (conductivity, temperature & depth) and additional  
10 sensors. Since CTD data during ISL\_00314 does not meet all quality control measures  
11 following GO-SHIP standards we expect for the hydrographic data an accuracy of about twice  
12 the GO\_SHIP standard, which is for temperature 0.002°C, for salinity 0.004 and for oxygen  
13 sensor data approx. 4  $\mu\text{mol kg}^{-1}$  (note that M105 data fulfil these criteria).

14 Along with CTD casts, an underwater vision profiler 5 (UVP, Picheral et al., 2010) was  
15 deployed during both cruises in order to quantify particle distribution in the water column (see  
16 results in Hauss et al., 2015). During both cruises, CTD casts down to 600 m were performed  
17 and trying to survey as close as possible to the eddy core (guided by the near-real time  
18 satellite SLA maps) and likewise outside of the eddy to be able to investigate the horizontal  
19 contrast of the eddy to the surrounding waters. Based on the SLA data the “outside stations”  
20 during ISL and M105 were located 43 and 54 kilometres away from the supposed eddy  
21 centre, respectively. It however turned out that these stations were probably more at the rim  
22 of the eddy than in the surrounding water representing typical background conditions. In order  
23 to compare the eddy observations to the typical background conditions we used data collected  
24 during M105 at the CVOO time series station (see section 2.2).

25 Additionally, a section across the eddy was performed during M105 that included multiple  
26 hydrocasts (CTD/UVP-only, no bottle sampling) as well as current and backscatter profiles  
27 with the ship-borne Acoustic Doppler Current Profiler (ADCP) instrument and vertically  
28 stratified plankton net hauls (see results in Hauss et al., 2015).

29 For comparison, we also used data from an Argo profiling float (WMO no. 6900632) that got  
30 trapped in a low-oxygen cyclonic eddy (Karstensen et al., 2015; Ohde et al., 2015). This float  
31 was equipped with an oxygen sensor (AADI Aanderaa optode 3830) and a transmissometer



1 (CRV5, WETLabs). The given uncertainties of the float measurements were  $\pm 2.4$  dbar for  
2 pressure,  $\pm 0.002^\circ\text{C}$  for temperature and  $\pm 0.01$  for salinities. The float was deployed in  
3 February 2008 at the Mauritanian shelf edge and propagated in a rather straight, west-  
4 northwest course, into the open waters of the ETNA.

## 5 **2.2 Reference Data Sets**

6 Data from former research expeditions in the ETNA, conducted in other research programs  
7 (e.g., SOPRAN, SOLAS, SFB 754), were used to put the results of the dedicated eddy  
8 surveys into regional context. For the Mauritanian shelf area (Figure 1) three cruises were  
9 identified that sampled the region during that part of the year when eddies are typically  
10 created (and so was the target eddy) and released to the open Atlantic Ocean (Schütte et al.,  
11 2015): RV Meteor cruise M68-3 (12 July – 6 August 2006) conducted a biogeochemical  
12 survey from the Mauritanian Upwelling region up to the Cape Verde Archipelago, RV  
13 Poseidon cruise POS399/2 (31 May – 17 June 2010) which operated in the same area and RV  
14 Meteor cruise M107 (29 May – 03 July 2014) focused on benthic biogeochemical processes  
15 along the Mauritanian shelf edge. Data from selected stations near the shelf edge from all  
16 three cruises were used as a reference for biogeochemical characteristics during the eddy  
17 formation.

18 Likewise, representative background conditions for the actual survey area northwest of the  
19 Cape Verde Islands were estimated from data collected during M105 at the near-by CVOO  
20 ( $17.58^\circ\text{N}$ ,  $-24.28^\circ\text{E}$ , Figure 1). The observatory includes a ship-based sampling program and  
21 a mooring (Fischer et al., 2015; Karstensen et al., 2015) and is located about 167 kilometres  
22 south of the eddy survey location (at the time of the ISL sampling) in an open-ocean setting.  
23 We used data of the CVOO sampling during M105 as background conditions in order to  
24 illustrate local biogeochemical anomalies caused by this ACME.

## 25 **2.3 Analytical Methods**

26 All discrete seawater samples collected for this study were analyzed for dissolved oxygen  
27 after Hansen (2007) with manual end-point determination. Samples were stored dark after  
28 sampling and fixation and were analyzed within 12h on board. Regular duplicate  
29 measurements were used to ensure high precision of measurements (ISL:  $0.27 \mu\text{mol kg}^{-1}$ ,



1 M105:  $0.34 \mu\text{mol kg}^{-1}$ ). Oxygen bottle data were also used to calibrate the oxygen sensors  
2 mounted on CTD instruments.

3 Samples for nutrients were analyzed with autoanalyzer systems following the general method  
4 by Hansen and Koroleff (2007). Nutrient samples during ISL and M105 surveys were always  
5 taken as triplicates, stored at  $-20 \text{ }^\circ\text{C}$  immediately after sampling and were analyzed onshore  
6 within 3 weeks (ISL) and 2 months (M105) after collection, respectively. Obtained precisions  
7 from regular triplicate measurements (in  $\mu\text{mol kg}^{-1}$ ) for nutrient analyses were 0.08 (nitrate),  
8  $<0.01$  (nitrite), 0.02 (phosphate), 0.04 (silicate) for ISL and 0.08 (nitrate), 0.02 (nitrite), 0.05  
9 (phosphate) and 0.07 (silicate) for M105.

10 Samples for dissolved inorganic carbon (DIC) and total alkalinity (TA) were preserved and  
11 stored for later onshore analysis, following procedures recommended by Dickson et al.  
12 (2007). Briefly, 500 mL borosilicate glass bottles were filled air bubble-free with seawater  
13 and then poisoned with 100  $\mu\text{L}$  of saturated mercuric chloride solution. Samples were stored  
14 at room temperature in the dark and in case of later onshore analysis shipped to GEOMAR for  
15 analysis within 3 month after sampling. Preserved samples as well as samples directly  
16 analyzed onboard were measured using automated high precision analyzing systems  
17 performing a coulometric titration for DIC (SOMMA, Johnson et al. 1993) and a  
18 potentiometric titration for TA (VINDTA, Mintrop et al. 2000). High quality of obtained  
19 results was ensured by regular measurements of certified reference material (CRM, A.  
20 Dickson, Scripps Institution of Oceanography, La Jolla, USA; Dickson, 2010) and duplicate  
21 samples (TA:  $1.30 \mu\text{mol kg}^{-1}$ , DIC:  $1.45 \mu\text{mol kg}^{-1}$ ). Results from DIC and TA analysis were  
22 used to compute the remaining parameters of the marine carbonate system (pH,  $p\text{CO}_2$  and  
23  $\Omega_{\text{Ar}}$ ) using carbonic acid dissociation constants after Mehrbach et al. (1973) as refitted by  
24 Dickson and Millero (1987).

25 Samples for DOC/DON were collected into combusted (8 h,  $500^\circ\text{C}$ ) glass ampules after  
26 passing through combusted (5 h,  $450^\circ\text{C}$ ) GFF filters and acidified by an addition of 80  $\mu\text{L}$  of  
27 80% phosphoric acid. The DOC was analysed with the high-temperature catalytic oxidation  
28 method adapted after Sugimura and Suzuki (1988). Total dissolved nitrogen (TDN) was  
29 determined simultaneously to DOC using a TNM-1 detector on Shimatzu analyser. DON  
30 concentrations were further calculated by subtraction of measured total inorganic nitrogen  
31 ( $\text{NO}_3^- + \text{NO}_2^-$ ) from TDN. The calibrations and measurements are described in more detail in  
32 Loginova et al. (2015) and Engel and Galgani (2015).



1 Filtration of seawater (1 L of seawater <150 m and 2 L >150 m depth) through a GFF filter  
2 (0.8  $\mu\text{m}$  pore size) was conducted during M105 in order to determine particulate fractions of  
3 organic carbon and nitrogen. Filters were stored frozen (-20 °C) until analyses. In the lab,  
4 filters were exposed to fuming hydrochloric acid to remove inorganic carbon, dried at 60°C  
5 for ~6 hours, wrapped in tin foil and processed in an Euro EA elemental analyzer calibrated  
6 with an acetanilide standard.

7

## 8 **2.4 Oxygen Utilization**

9 Karstensen et al. (2015) suggested that the low-oxygen cores of the eddies were created from  
10 an enhanced respiration due to high surface productivity and subsequently sinking of  
11 particulate matter combined with reduced oxygen supply (due to an efficient isolation of the  
12 core from surrounding waters). The high productivity is proposed to be driven by vertical  
13 nutrient flux into the euphotic zone, a situation that resamples coastal upwelling regions.  
14 Therefore we compare our results of the analysis of the eddy in spring 2014 (e.g., production  
15 and respiration of organic matter and related export fluxes) with observations from the  
16 Mauritanian shelf.

17 Based on satellite SLA data the formation location of the target eddy is reconstructed to be  
18 close to the shelf edge off Mauritania at approx. 18°N (Figure 1). This is further corroborated  
19 by an elaborate statistical analysis of historical SLA data (Schütte et al., 2015) which  
20 identified this region as one hotspot for the creation of anticyclonic mode water eddies  
21 (ACMEs). We used the station data (CTD hydrocasts and discrete water sampling) from the  
22 three cruises mentioned above which fall into the area 17.45 °N to 18.55 °N and -17.10 °E to -  
23 16.45 °E (Figure 1). In order to account for small-scale variability of water column properties  
24 within this area, an average profile for each investigated parameter was created by averaging  
25 on isopycnals but mapped back to depth via the mean depth/density profile. These mean  
26 profiles were assumed to reflect typical initial conditions of ACMEs during formation in the  
27 Mauritanian shelf area in boreal summer (Table 1).

28 This reference data from the shelf was then used to determine the changes in biogeochemical  
29 parameters en route from the formation to the survey area northwest of Cape Verde. Again,  
30 the anomalies were determined along isopycnals and mapped back to depth. We assume that  
31 the core of the eddy was not significantly affected by either horizontal or vertical mixing as





1 such ACMEs are known to host highly isolated water bodies due to their physical structure  
 2 (Karstensen et al., 2015). This assumption allows us to derive estimates for biogeochemical  
 3 rates being independent of mixing processes.

4 In order to determine the apparent oxygen utilization rate (aOUR) and the carbon  
 5 mineralization rate (CRR) not only the anomaly but the “age” of the eddy, that is the time  
 6 between formation on the shelf and the time the eddy surveys took place, needs to be known.  
 7 The age was determined from the SLA tracking algorithm, that was also used to determine the  
 8 area of origin (Schütte et al., in prep. for this issue; Figure 1). Biogeochemical rates were then  
 9 estimated along multiple isopycnal surfaces between the shelf and the eddy interior as shown  
 10 here for determination of CRRs:

$$\text{CRR}_i = \frac{\text{DIC}_{E,i} - \text{DIC}_{S,i}}{t_E - t_S} \quad (1)$$

11 where  $\text{CRR}_i$  is the carbon remineralization rate along the isopycnal surface  $i$ ,  $\text{DIC}_{E,i}$  the  
 12 observed DIC concentration within the eddy on isopycnal  $i$ ,  $\text{DIC}_{S,i}$  the average DIC  
 13 concentration on the shelf on isopycnal  $i$ ,  $t_E$  the time of the eddy survey, and  $t_S$  the back-  
 14 calculated time the eddy was created in the shelf area. The same approach was followed to  
 15 determine rates for all other available biogeochemical variables as well.

16 Data from the Argo float trapped inside a CE in 2008 was processed as described in  
 17 Karstensen et al. (2015). Corresponding CRRs were derived from aOURs by applying a  
 18 Redfield stoichiometric ratio of  $-\text{O}_2:\text{C}_{\text{org}} = 1.34 \pm 0.06$  (Körtzinger et al., 2001a) as no direct  
 19 measurements of the carbonate system exist for this CE.

## 20 2.5 Carbon Export Flux

21 We used CRR to estimate the shape of the vertical export flux curve for particulate organic  
 22 carbon (POC) out of the euphotic zone which is generally being described by the established  
 23 Martin Curve (Martin et al., 1987a):

$$F(z) = F_{100} \cdot \left(\frac{z}{100}\right)^{-b} \quad (2)$$

24 where  $F(z)$  is the POC flux at a given depth  $z$ ,  $F_{100}$  the corresponding export flux at 100 m and  
 25  $b$  a unitless fitting parameter that describes the shape of the curve.



1  $F_{100}$  can be determined following an approach by Jenkins (1982) using a log-linear aOUR-  
2 depth dependence which can be also described for CRR as follows:

$$\ln(\text{CRR}) = m \cdot z + c \quad (3)$$

3 where  $m$  is the slope and  $c$  the intercept of the linear regression of  $\ln(\text{CRR})$  versus depth. An  
4 estimate for  $F_{100}$  can be obtained by vertically integrating  $F(z)$  from 100 m downward to a  
5 maximum depth  $a$ :

$$F_{100} = \int_{100}^a \ln(\text{CRR}) dz = \int_{100}^a e^{(m \cdot z + c)} dz \quad (4)$$

6 The  $b$  parameter of the Martin equation (eq. (2)) can then be determined as the slope of the  
7 linear regression of  $\ln(\text{CRR})$  on  $\ln(z)$ .

8 The rates we derive assume that the changes can exclusively be ascribed to the  
9 biogeochemical processes and no transport processes (ventilation) play a role. As such  
10 reported rates in this study are to be seen as lower order estimates. However, from the  
11 comparison of the hydrographic properties in the eddy formation area and the survey area this  
12 assumption is plausible for the core of the eddy (see detailed discussion in section 3.1).

13

### 14 **3 Results & Discussion**

15 In the following sections, we first examine the hydrographic (section 3.1) and biogeochemical  
16 setting (sections 3.2 - 3.4) of the surveyed ACME in a phenomenological sense. In order to  
17 better understand and interpret the biogeochemical anomalies found in the eddy core we  
18 compare our results with observations that are representative for either the Mauritanian shelf  
19 region or the ambient open-ocean conditions outside of the eddy. We then derive estimates for  
20 aOUR and carbon export rates from these data.

#### 21 **3.1 Hydrography**

22 The Temperature-salinity (TS) characteristics of the core of ACMEs in the open ETNA  
23 (Schütte et al., in prep. for this issue; Karstensen et al., 2015) were found to be nearly  
24 unchanged, compared to coastal regions. They resample South Atlantic Central Water  
25 (SACW), the predominating upper layer water mass in the Mauritanian Upwelling region.  
26 Towards the west and north, the influence of SACW decreases and is taken over by North  
27 Atlantic Central Waters (NACW), the dominant water mass of the ventilated part of the North



1 Atlantic subtropical gyre (Pastor et al., 2008). As expected for a low-oxygen eddy, the TS  
2 characteristic in the 2014 eddy core for the two surveys matches very well with the  
3 characteristic found from the Mauritanian shelf reference stations (Figure 2), thereby  
4 underlining the isolation of the eddy against mixing processes with surrounding waters during  
5 its westward propagation from the shelf into the open. However, below the eddy core  
6 ( $\sigma_{\theta} > \sim 26.6 \pm \sim 250$  m) TS characteristics become more variable and no indication for isolation  
7 is found. The upper bound of the eddy core is the mixed layer base, characterized by a very  
8 sharp gradient (between 70 – 77 m depth) in all parameters. The vertical contrast amounts to  
9 0.73 in salinity, 3.98°C in temperature and 165.8  $\mu\text{mol kg}^{-1}$  in dissolved oxygen. As expected  
10 from the satellite analysis of Schütte et al. (2015), the mixed layer temperature were found to  
11 differ significantly from outside-eddy conditions. Underway measurements of temperature  
12 recorded at 5 m depth during M105 reveal colder temperatures within the eddy when  
13 compared to outside conditions.

### 14 3.2 Oxygen and Nutrients

15 Despite quasi-constant physical water mass properties over the course of the eddy's lifetime,  
16 changes in biogeochemical variables are observed. Continuing processes such as biological  
17 production in the euphotic zone and organic matter respiration within the low-oxygen core as  
18 well as underneath drive significant changes in biogeochemical properties over time. In  
19 comparison to the reference profile from the Mauritanian Shelf we find a maximum oxygen  
20 decrease in the eddy core (100 m) of about 57.0  $\mu\text{mol kg}^{-1}$  to suboxic levels ( $< 5 \mu\text{mol kg}^{-1}$ ;  
21 Figure 3). We expect the oxygen decrease from continuous respiration of the organic material  
22 that sinks out of the euphotic zone into an environment that is only minimal affected by lateral  
23 ventilation of the eddy waters. A more detailed assessment of oxygen utilization is presented  
24 in section 3.5.

25 We observe elevated nutrient concentrations (nitrate, phosphate, silicate) inside the ACME  
26 which indicate the remineralization of organic matter (Figure 4). Nutrient data obtained  
27 during the ISL survey showed also elevated concentrations for nitrate, nitrite and phosphate in  
28 the mixed layer of the eddy. Such elevated surface nutrient concentrations are untypical for  
29 the oligotrophic waters of the open ETNA but can be observed in the coastal upwelling region  
30 (Löscher et al., 2015). As such, we expect them to be a signature of a vertical flux event. As  
31 these elevated surface concentrations were not found during the M105 sampling we expect  
32 that the upwelling is intermittent and/or maybe occur only locally, confined to certain regions



1 across the eddy. In any case, the upwelled nutrients fuel surface production, which, in turn,  
2 draws down nutrient levels quickly again. In an oligotrophic ocean setting such an eddy with  
3 sporadic upwelling events creates a significant anomaly when compared to ambient  
4 conditions. Consequences on carbon cycling and sequestration are discussed in next sections  
5 in more detail.

### 6 3.3 Carbonate System

7 By using the measured DIC and TA, the remaining two parameters of the marine carbon cycle  
8 (pH and  $p\text{CO}_2$ ) as well as saturation levels for Aragonite ( $\Omega_{\text{Ar}}$ ) have been calculated following  
9 methods described in section 2.3. In accordance with the oxygen decrease already discussed, a  
10 clear respiration signal was also found in carbon parameters (Figure 5). Values for DIC (max.  
11  $2258.8 \mu\text{mol kg}^{-1}$ ) and  $p\text{CO}_2$  (max.  $1163.9 \mu\text{atm}$ ) as well as for pH (min. 7.63) in the core of  
12 the eddy deviate significantly from those observed in the reference profiles from the  
13 Mauritanian Shelf region where the eddy was formed. Moreover, these values can be seen as  
14 the highest or lowest end members for the open ETNA, respectively, thus creating an extreme  
15 biogeochemical environment on the mesoscale. One parameter that illustrates this contrasting  
16 environment very well is  $\Omega_{\text{Ar}}$  which inside the eddy core dropped to 1.0 (i.e. the threshold  
17 below which carbonate dissolution is thermodynamically favored; Figure 5). This value is  
18 very much in contrast to the regional background conditions at CVOO where  $\Omega_{\text{Ar}}=1$  is found  
19 below 2500 m depth and the typical  $\Omega_{\text{Ar}}$  at 100 m depth is approx. 2.4.

20 The horizontal gradient of pH between inside and outside eddy conditions is up to 0.3 pH  
21 units at a water depth of approx. 100 m. It is interesting to note that a pH of 7.63 is close to  
22 values expected for future surface ocean conditions in the year 2100 (approx. pH of 7.8) as  
23 predicted by models assuming a global high  $\text{CO}_2$  emission scenario (Bopp et al., 2013).  
24 Further, such low pH levels are used for example in artificial mesocosm experiments to  
25 simulate these future conditions (REFERENCE!!!). Absolute values of pH inside the eddy  
26 exceed these predictions and plankton communities inside the OMZ core are exposed to these  
27 acidified conditions. Vertically migrating zooplankton and nekton also encounter such a  
28 pronounced gradient during migration (see Hauss et al., 2015).

29 Above the core, DIC concentrations in the surface mixed layer vary between the two eddy  
30 surveys and CVOO. Slightly higher values were found during the ISL survey when compared  
31 to the M105 survey. The same was found for nutrient concentrations (section 3.2), which



1 consistently points towards a very recent or even ongoing upwelling event encountered during  
2 the ISL sampling. Episodic upwelling within ACMEs have been reported for other regions in  
3 the past (McGillicuddy et al., 2007).

4 Below the eddy core at a depth of approx. 200 m, the DIC anomaly disappears and parameters  
5 fall back close to shelf background conditions (Figure 5). A slightly different picture is found  
6 in profile data for TA. Here, only a minor change in TA inside the eddy core is found. This  
7 was expected as respiration processes have a small but significant effect on TA (Wolf-  
8 Gladrow et al., 2007). However, the major difference at depth (increased values for TA inside  
9 the core compared to shelf background) cannot be accounted for by respiration. One potential  
10 reason for this pattern is calcium carbonate dissolution at depth. This explanation, however,  
11 can be excluded since both  $\Omega_{Ar}$  is too high at these depths and aragonite dissolution would  
12 also positively affect DIC concentrations (the increase of which can essentially be explained  
13 by respiration). Thus, the more likely explanation is an intrusion of ambient NACW waters,  
14 which, considering distinct TA-salinity relationships (Lee et al., 2006), would also affect TA  
15 concentrations towards elevated levels. Indeed, vertical profiles for salinity (Figure 3) show  
16 slightly higher salinity values beneath the eddy core. Furthermore, TA-salinity correlations  
17 show different patterns when comparing between the eddy core and underneath (data not  
18 shown) which also corroborates this interpretation.

### 19 **3.4 Particles and Organic Matter**

20 We used data from the UVP to illustrate vertical distribution of small particles (60 – 530  $\mu\text{m}$ )  
21 in the water column. Particle abundances show a peak at subsurface depth within the shallow  
22 OMZ slightly below the oxygen minima observed during the ISL and M105 surveys (Figure  
23 6). This points at accumulated particles fueling microbial respiration in the core of the eddy.  
24 Furthermore, surface concentrations of particles significantly exceed open-ocean conditions  
25 as found at CVOO. This is in line with Löscher et al. (2015) who described a threefold higher  
26 primary production for surface waters inside the eddy as compared to the outside. In the  
27 Mauritanian shelf area particle concentrations are much higher throughout the water column.  
28 Enhanced biological production as well as influence from nepheloid layers (Fischer et al.,  
29 2009; Ohde et al., 2015) along the shelf edge most likely cause this high level of particle  
30 abundance. According to Hauss et al. (2015) large aggregates (>500 $\mu\text{m}$  equivalent spherical  
31 diameter, UVP data) are 5-fold more abundant in the upper 600 m within the eddy than in the  
32 usual open ocean situation in this region, suggesting a substantial increase in export flux.



1 Discrete bottle samples for organic carbon (POC, DOC) and nitrogen (PON, DON) were  
2 collected during the M105 survey only (Figure 6). Both POC and DOC concentrations are  
3 elevated inside the eddy compared to concentrations found at CVOO. In particular, POC  
4 shows a major peak in the surface mixed layer that exceeds not only concentrations at CVOO  
5 but also all other POC concentrations measured during the M105 cruise (including data  
6 between Cape Verde and 7°N, data not shown). A similar picture was found for PON  
7 concentrations. Again, these observations match very well with the findings by Löscher et al.,  
8 (2015). Within the eddy core, only a very minor (positive) peak in POC (and PON) appears  
9 which is located somewhat beneath the actual oxygen minimum of the core. Data below  
10 250 m then match well with background conditions again. Vertical profiles for DOC (and  
11 DON) also show higher values in the surface as well as a distinct (positive) peak beneath the  
12 oxygen minimum. In contrast to the particulate fraction, DOC (DON) concentrations at depth  
13 exceed background conditions. The position of the small POM and the pronounced DOM  
14 peaks beneath the actual oxygen minimum is confirmed by UVP particle data (one should  
15 note that the depth of the UVP particle peak is slightly shallower than the associated discrete  
16 sample). The obvious minimum in DOM exactly at the oxygen minimum (Figure 6) suggests  
17 prolonged bacterial consumption of DOM at this depth. In other words, the drawdown of  
18 POM and DOM by bacterial respiration can be already observed right beneath the  
19 oxycline/mixed layer base at approx. 70 m depth and intensifies towards the core of the eddy  
20 at approx. 98 m (during the M105 survey). Below the eddy core, along with POM and DOM  
21 peaks, an accumulation of particles with low nucleic acids content was determined (Loginova,  
22 pers. comm.). These particles might represent ruptured or dead bacterial cells. Therefore cell  
23 mortality could induce a release of organic matter at this depth. However, the abrupt  
24 accumulation of particulate matter (UVP profiles, and, to a lesser extent, discrete POM data)  
25 and DOM somewhat beneath the core remains speculative so far.

### 26 **3.5 Oxygen Utilization & Carbon Export**

27 Based on the differences between the observed concentrations in the eddy and the reference  
28 profiles in the Mauritanian upwelling region the oxygen and DIC changes and respective rates  
29 (section 2.4) were estimated (Figure 7). As outlined before, the data was compared in density  
30 space in order to consider the large scale differences in the depth/density relation that  
31 primarily reflects the difference in ocean dynamics (Figure 7, larger panels). As outlined in  
32 section 2.4, the corresponding rates, presented here against depth (Figure 7, smaller panel),



1 were then calculated based on the estimated lifetime of the eddy (derived from satellite data).  
2 Thus, examined rates represent mean rates over the lifetime of the eddy and do not contain  
3 any information about their temporal evolution.

4 Data show clear anomalies for all parameters within the eddy core which were most  
5 pronounced at a depth of 98 m (M105) and 105 m (ISL), respectively. Rates for all parameters  
6 are presented in Table 1. Below the eddy core, however, rates are vanishing and become  
7 indistinguishable from the uncertainty introduced by the applied isopycnal approach. For  
8 instance, the assumption of a well isolated water body holds true for the core of the eddy only,  
9 but not necessarily for deeper parts of the eddy. Here, admixture of ambient waters becomes  
10 more likely in agreement with the TS characteristic approaching the background signature  
11 (Figure 2), which significantly alters water mass properties of this part of the eddy. As a  
12 consequence of the non-isolation of the water underneath the core (below approx. 250 m)  
13 rates can not be derived using this approach and not further discussed. Similarly, rates can  
14 also be not derived for the surface mixed layer were multiple processes modify the parameter  
15 field (gas, heat and freshwater exchange).

16 The apparent oxygen utilization rate (aOUR) within the eddy peaks at  $0.26 \mu\text{mol kg}^{-1} \text{d}^{-1}$   
17 (M105 survey) in the oxygen minimum which corresponds to the  $\sigma_{\theta} = 26.35$  isopycnal. This  
18 aOUR is one of the highest values which have been reported so far for the ETNA. Karstensen  
19 et al. (2008) derived large scale thermocline aOUR from transient tracer data and AOU values  
20 and found a mean aOUR of  $0.03 \mu\text{mol kg}^{-1} \text{d}^{-1}$  in the similar depth range (similar to other  
21 estimates such as Jenkins 1982). However, from a low-oxygen CE a direct estimate based on  
22 an Argo float that was trapped in an eddy revealed 3 to 5 times higher rates (Karstensen et al.,  
23 2015). In the same study, an aOUR of  $0.25 \mu\text{mol kg}^{-1} \text{d}^{-1}$  within another ACME was found  
24 based on an approach similar to ours by comparing oxygen in the upwelling region with the  
25 oxygen concentrations 7 months later. The smaller rates found in the cyclonic eddy might  
26 indicate a less isolated core but could also be related to the steady mixed layer deepening in  
27 the CE which may provide a diapycnal oxygen pathway. However, in summary aOUR within  
28 CEs as well as ACMEs significantly exceed typical rates in the ETNA.

29 Rate estimates for other biogeochemical parameters within the investigated ACME are also  
30 exceptionally high (Table 1). We compared estimated rates with each other by looking at  
31 stoichiometric ratios such as C:N, N:P and -O:C (data not shown). In fact, all ratios were  
32 found to be close to, or not distinguishable from, the stoichiometry proposed by Redfield et al.



1 (1963). This finding provides indication for a reliable assessment of biogeochemical rates  
2 based on the assumptions that were made and on independent samples of multiple parameters  
3 taken during two independent cruises.

4 The observed DIC increase rate within the eddy core can be referred to as the CRR resulting  
5 from continued respiration of organic matter. As illustrated in Figure 5, the peak in DIC  
6 coincides with the depth of the sharpest decrease of POM and DOM. This is to be expected,  
7 as the CRR should equal the derivative of the vertical POC flux curve with respect to the  
8 depth. Following the approach of Jenkins (1982) one can derive the vertical flux of POC from  
9 aOUR or CRR values, respectively. Downward fluxes for POC can be seen as the major  
10 export process of carbon out of the euphotic zone.

11 We used these CRRs within the eddy core for determination of the vertical POC flux at  
12 different depths by means of a power law function (Martin et al., 1987b). Vertical integration  
13 of the data between 100 m and 1000 m yielded estimates of the vertical POC flux at 100 m  
14 during the ISL and M105 cruises of  $0.19 (\pm 0.08)$  and  $0.23 (\pm 0.15) \text{ g C m}^{-2} \text{ d}^{-1}$ , respectively  
15 (Figure 8). These values are exceptionally high both for the ETNA but also for other open-  
16 ocean regions. Table 2 provides a brief overview of studies that determined POC fluxes at  
17 different locations based on different methods. In the open ETNA, recently determined POC  
18 fluxes at 100 m from floating sediment trap deployments (Wagner et al., pers. comm.) were  
19 lower by a factor of approx. 3 than inside the ACME. Interestingly, the same authors revealed  
20 POC fluxes at the Mauritanian shelf edge in the same magnitude as found inside the  
21 investigated ACME. This supports the view that these ACMEs can be viewed as isolated,  
22 westwards propagating upwelling systems as their own.

23 POC fluxes derived here generally show higher values than found in other open-ocean studies  
24 but are comparable to values associated with a North Atlantic spring bloom event (Berelson,  
25 2001). Moreover, POC fluxes for this ACME were also in line with estimates made for other  
26 eddies, such as enhanced POC fluxes determined at the rim of a CE in the Western Pacific  
27 (Shih et al., 2015) or inside a CE in the ETNA (Figure 8, derived from aOUR data in  
28 Karstensen et al., 2015). In general, estimated POC fluxes for the surveyed ACME based on  
29 the method described in section 2.5 may represent a rather conservative estimate as the aOUR  
30 was derived based on the assumption of complete absence of vertical and horizontal  
31 ventilation processes. Thus, any minor ventilation process affecting the eddy core would  
32 cause our OURs and POC flux estimates to be biased low.





1 The corresponding  $b$  parameter of the Martin curve for the two ACME surveys are high (1.55  
2 – 1.64, Figure 8) when compared with typical open-ocean values. High  $b$  values indicate steep  
3 and thus local flux attenuation in the upper layer which, in our case, could be explained by the  
4 vertical structure of the ACME with its well-isolated local core. Again, our findings for flux  
5 attenuation are comparable to those obtained during a North Atlantic bloom experiment  
6 (Berelson, 2001) but also to observations recently conducted in the North Atlantic subtropical  
7 gyre (Marsay et al., 2015). Controversial discussions in the scientific literature exist about  
8 different dependencies of the  $b$  parameter. For instance, Marsay et al. (2015) also compared  
9 POC flux determinations from four different sites in the North Atlantic with each other. They  
10 found a positive correlation between water temperature and the  $b$  parameter in the North  
11 Atlantic. Berelson (2001) proposed a linear relationship between the POC flux at 100 m and  
12 the  $b$  parameter which also matches with our data. In contrast, a few studies also suggest a  
13 dependency between the  $b$ -parameter and ambient oxygen concentrations with lower  $b$ -values  
14 found in low oxygen environments (Devol and Hartnett, 2001; Van Mooy et al., 2002). Our  
15 data do not reflect this relationship, most likely due to physical processes inside the eddy such  
16 as local upwelling and redistribution of particulate matter which may alter the shape of the  
17 downward POC flux. Since we are lacking direct flux measurements and only have a very  
18 limited number of observations we are not able to appropriately de-convolve drivers of the  
19 derived POC flux attenuation profile inside this ACME.

20

#### 21 **4 Conclusions**

22 We performed two biogeochemical surveys within an ACME in the open ETNA off West  
23 Africa near the CVOO time-series site. The core of this mesoscale eddy was found to host an  
24 extreme biogeochemical environment just beneath the surface mixed layer. The concentration  
25 of oxygen had dropped to suboxic levels as a consequence of severely hindered vertical and  
26 horizontal ventilation of the core along with continuing remineralization during the eddy's  
27 lifetime. There is evidence that moderately elevated nutrient concentrations in the top layer of  
28 the ACME are caused by (episodic) upwelling events and fuel an enhanced surface primary  
29 productivity that moves with the ACME. Likewise, nutrient concentrations as well as  $p\text{CO}_2$   
30 levels showed an intense increase which created significant anomalies when compared to  
31 ambient open-ocean ETNA conditions. Values of pH, for instance, indicate highly acidified  
32 waters at the lower edge of the euphotic zone which corresponds to  $\Omega_{\text{Ar}}$  values of 1.



1 We also investigated magnitudes of biogeochemical processes occurring within the eddy  
2 during its westward propagation such as apparent oxygen utilization and carbon  
3 remineralization by comparing our survey data with conditions prevailing during the ACME's  
4 initial state (Mauritanian shelf). Results showed mean aOURs over the lifetime of the ACME  
5 that exceed typical rates in the open-ocean ETNA by an order of magnitude (Karstensen et al.,  
6 2008). Resulting POC fluxes inside the ACME was also found to exceed background fluxes  
7 in the oligotrophic ETNA by a factor of two to three and thus are comparable to meso- and  
8 eutrophic regions such as the Mauritanian upwelling region or the subpolar North Atlantic  
9 spring bloom. This finding is also in line with a three-fold enhanced primary productivity in  
10 the same ACME's surface layer derived from Löscher et al. (2015) based on seawater  
11 incubations. Our results confirm that ACMEs in the ETNA can be seen open-ocean outposts  
12 that clearly exhibit their origin in the EBUS but through their continued biogeochemical  
13 activity at the same time represent alien biogeochemical environments in a subtropical ocean  
14 setting.

15 The results of this study, however, are based on two independent surveys carried out at a  
16 certain point of time in the lifetime of the ACME. Thus, we are not able to address questions  
17 about the evolution and (non-) linearity of processes within the ACME throughout its lifetime.  
18 Therefore, future surveys should resolve not only spatial structure but also temporal evolution  
19 of biogeochemical processes at different life stages of these eddies.

20 In addition to this biogeochemical investigation, two other studies have documented the  
21 impacts of this low-oxygen ACME on zooplankton and microbial communities (Haus et al.,  
22 2015; Löscher et al., 2015). There is empirical indication that future scenarios such as  
23 deoxygenation and ocean acidification can also affect higher trophic species (Munday et al.,  
24 2010; Stramma et al., 2012). Any possible influence of this ACME on higher trophic levels,  
25 however, remains unknown and would require a different observational approach. The  
26 discovered anomalies within this eddy can be seen as a large (50-100 km diameter) and  
27 relatively long-lived (~1 year) mesocosm featuring the development of low-oxygen and low-  
28 pH conditions in a completely unmanipulated natural environment. Hence, investigating the  
29 full range of this mesocosm-ecosystem will provide useful data and may help to better  
30 understand ecosystem responses to future ocean conditions.

31

32



## 1 **Acknowledgements**

2 The authors would like to thank Meteor M105 chief scientists M. Visbeck and T. Tanhua for  
3 their spontaneous support of the “Eddy Hunt” project, as well as H. Bange and S. Sommer for  
4 providing hydrographic data for the Mauritanian shelf area. Conducting field work at Cape  
5 Verde would not have been possible without the tremendous support and engagement of the  
6 CVOO team at INDP (Ivanice Monteiro, Nuno Vieira and Carlos Santos) as well as S.  
7 Christiansen and T. Hahn. For DIC, TA, nutrient and DOC/TDN sample analysis we thank S.  
8 Fessler, M. Lohmann and J. Roa. Processing of CTD data was performed by G. Krahmann  
9 and S. Milinski. We also appreciate professional support from captains and crews of RV  
10 Islândia and RV Meteor.

11 This study received financial support from the Cluster of Excellence “Future Ocean” (grant  
12 no. CP1341, “Eddy Hunt”), the BMBF project SOPRAN (grant no. 03F0662A), the DFG  
13 Collaborative Research Centre 754 and the European Commission for FP6 and FP7 projects  
14 CARBOOCEAN (264879) and CARBOCHANGE (264879).

15



## 1 **References**

- 2 Altabet, M. A., Ryabenko, E., Stramma, L., Wallace, D. W. R., Frank, M., Grasse, P. and  
3 Lavik, G.: An eddy-stimulated hotspot for fixed nitrogen-loss from the Peru oxygen minimum  
4 zone, *Biogeosciences*, 9(12), 4897–4908, doi:10.5194/bg-9-4897-2012, 2012.
- 5 Baird, M. E., Suthers, I. M., Griffin, D. A., Hollings, B., Pattiaratchi, C., Everett, J. D.,  
6 Roughan, M., Oubelkheir, K. and Doblin, M.: The effect of surface flooding on the physical–  
7 biogeochemical dynamics of a warm-core eddy off southeast Australia, *Deep. Res. Part II*  
8 *Top. Stud. Oceanogr.*, 58(5), 592–605, doi:10.1016/j.dsr2.2010.10.002, 2011.
- 9 Berelson, W.: The Flux of Particulate Organic Carbon Into the Ocean Interior: A Comparison  
10 of Four U.S. JGOFS Regional Studies, *Oceanography*, 14(4), 59–67,  
11 doi:10.5670/oceanog.2001.07, 2001.
- 12 Bopp, L., Resplandy, L., Orr, J. C., Doney, S. C., Dunne, J. P., Gehlen, M., Halloran, P.,  
13 Heinze, C., Ilyina, T., Séférian, R., Tjiputra, J. and Vichi, M.: Multiple stressors of ocean  
14 ecosystems in the 21st century: projections with CMIP5 models, *Biogeosciences*, 10(10),  
15 6225–6245, doi:10.5194/bg-10-6225-2013, 2013.
- 16 Brandt, P., Bange, H. W., Banyte, D., Dengler, M., Didwischus, S.-H., Fischer, T.,  
17 Greatbatch, R. J., Hahn, J., Kanzow, T., Karstensen, J., Körtzinger, A., Krahnmann, G.,  
18 Schmidtke, S., Stramma, L., Tanhua, T. and Visbeck, M.: On the role of circulation and  
19 mixing in the ventilation of oxygen minimum zones with a focus on the eastern tropical North  
20 Atlantic, *Biogeosciences*, 12(2), 489–512, doi:10.5194/bg-12-489-2015, 2015.
- 21 Buesseler, K. O., Lamborg, C. H., Boyd, P. W., Lam, P. J., Trull, T. W., Bidigare, R. R.,  
22 Bishop, J. K. B., Casciotti, K. L., Dehairs, F., Elskens, M., Honda, M., Karl, D. M., Siegel, D.  
23 A., Silver, M. W., Steinberg, D. K., Valdes, J., Van Mooy, B. and Wilson, S.: Revisiting  
24 carbon flux through the ocean’s twilight zone., *Science*, 316(5824), 567–70,  
25 doi:10.1126/science.1137959, 2007.
- 26 Chaigneau, A., Eldin, G. and Dewitte, B.: Eddy activity in the four major upwelling systems  
27 from satellite altimetry (1992–2007), *Prog. Oceanogr.*, 83(1-4), 117–123,  
28 doi:10.1016/j.pocean.2009.07.012, 2009.
- 29 Chelton, D. B., Schlax, M. G. and Samelson, R. M.: Global observations of nonlinear  
30 mesoscale eddies, *Prog. Oceanogr.*, 91(2), 167–216, doi:10.1016/j.pocean.2011.01.002, 2011.



- 1 Devol, A. H. and Hartnett, H. E.: Role of the oxygen-deficient zone in transfer of organic  
2 carbon to the deep ocean, *Limnol. Oceanogr.*, 46(7), 1684–1690,  
3 doi:10.4319/lo.2001.46.7.1684, 2001.
- 4 Dickson, A., Sabine, C. and Christian (Eds.), J.: Guide to best practices for ocean CO<sub>2</sub>  
5 measurements, *PICES Spec. Publ.*, 3, 191 pp [online] Available from:  
6 <http://aquacomm.fcla.edu/1443/> (Accessed 15 July 2010), 2007.
- 7 Dickson, A. G.: Standards for Ocean Measurements, *Oceanography*, 23(3), 34–47 [online]  
8 Available from:  
9 [http://apps.isiknowledge.com/full\\_record.do?product=WOS&search\\_mode=GeneralSearch&](http://apps.isiknowledge.com/full_record.do?product=WOS&search_mode=GeneralSearch&qid=4&SID=P2PB3opf6cK0mPbeMfj&page=1&doc=1)  
10 [qid=4&SID=P2PB3opf6cK0mPbeMfj&page=1&doc=1](http://apps.isiknowledge.com/full_record.do?product=WOS&search_mode=GeneralSearch&qid=4&SID=P2PB3opf6cK0mPbeMfj&page=1&doc=1) (Accessed 8 October 2010), 2010.
- 11 Dickson, A. G. and Millero, F. J.: A comparison of the equilibrium constants for the  
12 dissociation of carbonic acid in seawater media, *Deep. Res. Part I Oceanogr. Res. Pap.*,  
13 34(10), 1733–1743, doi:DOI: 10.1016/0198-0149(87)90021-5, 1987.
- 14 Engel, A. and Galgani, L.: The organic sea surface microlayer in the upwelling region off  
15 Peru and implications for air–sea exchange processes, *Biogeosciences Discuss.*, 12(13),  
16 10579–10619, doi:10.5194/bgd-12-10579-2015, 2015.
- 17 Falkowski, P. G., Ziemann, D., Kolber, Z. and Bienfang, P. K.: Role of eddy pumping in  
18 enhancing primary production in the ocean, *Nature*, 352(6330), 55–58 [online] Available  
19 from: <http://dx.doi.org/10.1038/352055a0>, 1991.
- 20 Fischer, G., Reuter, C., Karakas, G., Nowald, N. and Wefer, G.: Offshore advection of  
21 particles within the Cape Blanc filament, Mauritania: Results from observational and  
22 modelling studies, *Prog. Oceanogr.*, 83(1-4), 322–330, doi:10.1016/j.pocean.2009.07.023,  
23 2009.
- 24 Fischer, G., Karstensen, J., Romero, O., Baumann, K.-H., Donner, B., Hefter, J., Mollenhauer,  
25 G., Iversen, M., Fiedler, B., Monteiro, I. and Körtzinger, A.: Bathypelagic particle flux  
26 signatures from a suboxic eddy in the oligotrophic tropical North Atlantic: production,  
27 sedimentation and preservation, *Biogeosciences Discuss.*, 12(21), 18253–18313,  
28 doi:10.5194/bgd-12-18253-2015, 2015.
- 29 Gruber, N., Lachkar, Z., Frenzel, H., Marchesiello, P., Munnich, M., McWilliams, J. C.,  
30 Nagai, T. and Plattner, G.-K.: Eddy-induced reduction of biological production in eastern  
31 boundary upwelling systems, *Nat. Geosci.*, 4(11), 787–792 [online] Available from:



- 1 <http://dx.doi.org/10.1038/ngeo1273>, 2011.
- 2 Hansen, H. P.: Determination of oxygen, in *Methods of Seawater Analysis*, edited by K.
- 3 Grasshoff, K. Kremling, and M. Ehrhardt, pp. 75–89, Wiley-VCH Verlag GmbH. [online]
- 4 Available from: <http://dx.doi.org/10.1002/9783527613984.ch4>, 2007.
- 5 Hansen, H. P. and Koroleff, F.: Determination of nutrients, in *Methods of Seawater Analysis*,
- 6 edited by K. Grasshoff, K. Kremling, and M. Ehrhardt, pp. 159–228, Wiley-VCH Verlag
- 7 GmbH. [online] Available from: <http://dx.doi.org/10.1002/9783527613984.ch10>, 2007.
- 8 Hauss, H., Christiansen, S., Schütte, F., Kiko, R., Edvam Lima, M., Rodrigues, E.,
- 9 Karstensen, J., Löscher, C. R., Körtzinger, A. and Fiedler, B.: Dead zone or oasis in the open
- 10 ocean? Zooplankton distribution and migration in low-oxygen medewater eddies,
- 11 *Biogeosciences Discuss.*, 12(21), 18315–18344, doi:10.5194/bgd-12-18315-2015, 2015.
- 12 Jenkins, W. J.: Oxygen utilization rates in North Atlantic subtropical gyre and primary
- 13 production in oligotrophic systems, *Nature*, 300(5889), 246–248 [online] Available from:
- 14 <http://dx.doi.org/10.1038/300246a0>, 1982.
- 15 Johnson, K. M., Wills, K. D., Butler, D. B., Johnson, W. K. and Wong, C. S.: Coulometric
- 16 total carbon dioxide analysis for marine studies: maximizing the performance of an automated
- 17 gas extraction system and coulometric detector, *Mar. Chem.*, 44(2-4), 167–187,
- 18 doi:10.1016/0304-4203(93)90201-X, 1993.
- 19 Johnson, K. S., Berelson, W. M., Boss, E. S., Chase, Z., Claustre, H., Emerson, S. R., Gruber,
- 20 N., Körtzinger, A., Perry, M. J. and Riser, S. C.: Observing biogeochemical cycles at global
- 21 scales with profiling floats and gliders: prospects for a global array, *Oceanography*, 22, 216–
- 22 224 [online] Available from: <http://oceanrep.geomar.de/4040/>, 2009.
- 23 Karstensen, J., Stramma, L. and Visbeck, M.: Oxygen minimum zones in the eastern tropical
- 24 Atlantic and Pacific oceans, *Prog. Oceanogr.*, 77(4), 331–350 [online] Available from:
- 25 <http://www.sciencedirect.com/science/article/pii/S0079661108000670>, 2008.
- 26 Karstensen, J., Fiedler, B., Schütte, F., Brandt, P., Körtzinger, A., Fischer, G., Zantopp, R.,
- 27 Hahn, J., Visbeck, M. and Wallace, D.: Open ocean dead zones in the tropical North Atlantic
- 28 Ocean, *Biogeosciences*, 12(8), 2597–2605, doi:10.5194/bg-12-2597-2015, 2015.
- 29 Körtzinger, A., Koeve, W., Kähler, P. and Mintrop, L.: C:N ratios in the mixed layer during
- 30 the productive season in the northeast Atlantic Ocean, *Deep. Res. Part I Oceanogr. Res. Pap.*,



- 1 48(3), 661–688 [online] Available from:  
2 <http://www.sciencedirect.com/science/article/pii/S0967063700000510>, 2001a.
- 3 Körtzinger, A., Hedges, J. I. and Quay, P. D.: Redfield ratios revisited: Removing the biasing  
4 effect of anthropogenic CO<sub>2</sub>, *Limnology Oceanogr.*, 46(4), 964–970,  
5 doi:10.4319/lo.2001.46.4.0964, 2001b.
- 6 Lee, K., Tong, L. T., Millero, F. J., Sabine, C. L., Dickson, A. G., Goyet, C., Park, G.-H.,  
7 Wanninkhof, R., Feely, R. a. and Key, R. M.: Global relationships of total alkalinity with  
8 salinity and temperature in surface waters of the world's oceans, *Geophys. Res. Lett.*, 33(19),  
9 1–5, doi:10.1029/2006GL027207, 2006.
- 10 Loginova, A. N., Borchard, C., Meyer, J., Hauss, H., Kiko, R. and Engel, A.: Effects of nitrate  
11 and phosphate supply on chromophoric and fluorescent dissolved organic matter in the  
12 Eastern Tropical North Atlantic: a mesocosm study, *Biogeosciences*, 12(23), 6897–6914,  
13 doi:10.5194/bg-12-6897-2015, 2015.
- 14 Löscher, C. R., Fischer, M. A., Neulinger, S. C., Fiedler, B., Philippi, M., Schütte, F., Singh,  
15 A., Hauss, H., Karstensen, J., Körtzinger, A., Künzel, S. and Schmitz, R. A.: Hidden  
16 biosphere in an oxygen-deficient Atlantic open-ocean eddy: future implications of ocean  
17 deoxygenation on primary production in the eastern tropical North Atlantic, *Biogeosciences*,  
18 12(24), 7467–7482, doi:10.5194/bg-12-7467-2015, 2015.
- 19 Luyten, J. R., Pedlosky, J. and Stommel, H.: The Ventilated Thermocline, *J. Phys. Oceanogr.*,  
20 13(2), 292–309, doi:10.1175/1520-0485(1983)013<0292:TVT>2.0.CO;2, 1983.
- 21 Mahadevan, A.: Ocean science: Eddy effects on biogeochemistry, *Nature*, 506(7487), 168–  
22 169 [online] Available from: <http://dx.doi.org/10.1038/nature13048>, 2014.
- 23 Marsay, C. M., Sanders, R. J., Henson, S. A., Pabortsava, K., Achterberg, E. P. and Lampitt,  
24 R. S.: Attenuation of sinking particulate organic carbon flux through the mesopelagic ocean,  
25 *Proc. Natl. Acad. Sci.*, doi:10.1073/pnas.1415311112, 2015.
- 26 Martin, J. H., Knauer, G. A., Karl, D. M. and Broenkow, W. W.: VERTEX: carbon cycling in  
27 the northeast Pacific, *Deep. Res. Part I Oceanogr. Res. Pap.*, 34(2), 267–285,  
28 doi:10.1016/0198-0149(87)90086-0, 1987a.
- 29 Martin, J. H., Knauer, G. A., Karl, D. M. and Broenkow, W. W.: VERTEX: carbon cycling in  
30 the northeast Pacific, *Deep. Res. Part I Oceanogr. Res. Pap.*, 34(2), 267–285 [online]



- 1 Available from: <http://www.sciencedirect.com/science/article/pii/S0198014987900860>, 1987b.
- 2 McGillicuddy, D. J., Anderson, L. A., Bates, N. R., Bibby, T., Buesseler, K. O., Carlson, C.  
3 A., Davis, C. S., Ewart, C., Falkowski, P. G., Goldthwait, S. A., Hansell, D. A., Jenkins, W.  
4 J., Johnson, R., Kosnyrev, V. K., Ledwell, J. R., Li, Q. P., Siegel, D. A. and Steinberg, D. K.:  
5 Eddy/Wind Interactions Stimulate Extraordinary Mid-Ocean Plankton Blooms, *Science* (80-  
6 ), 316(5827), 1021–1026, doi:10.1126/science.1136256, 2007.
- 7 Mehrbach, C., Culberso, C. H., Hawley, J. E. and Pytkowic, R. M.: Measurement of Apparent  
8 Dissociation-Constants of Carbonic-Acid in Seawater at Atmospheric-Pressure, *Limnol.*  
9 *Oceanogr.*, 18(6), 897–907, 1973.
- 10 Mintrop, L., Perez, F. F., Gonzalez-Davila, M., Santana-Casiano, M. J. and Körtzinger, A.:  
11 Alkalinity determination by potentiometry: Intercalibration using three different methods,  
12 *Ciencias Mar.*, 26(1), 23–37, 2000.
- 13 Van Mooy, B. A. ., Keil, R. G. and Devol, A. H.: Impact of suboxia on sinking particulate  
14 organic carbon: Enhanced carbon flux and preferential degradation of amino acids via  
15 denitrification, *Geochim. Cosmochim. Acta*, 66(3), 457–465, doi:10.1016/S0016-  
16 7037(01)00787-6, 2002.
- 17 Munday, P. L., Dixson, D. L., McCormick, M. I., Meekan, M., Ferrari, M. C. O. and Chivers,  
18 D. P.: Replenishment of fish populations is threatened by ocean acidification, *Proc. Natl.*  
19 *Acad. Sci.* , 107 (29) , 12930–12934, doi:10.1073/pnas.1004519107, 2010.
- 20 Nagai, T., Gruber, N., Frenzel, H., Lachkar, Z., McWilliams, J. C. and Plattner, G.-K.:  
21 Dominant role of eddies and filaments in the offshore transport of carbon and nutrients in the  
22 California Current System, *J. Geophys. Res. Ocean.*, n/a–n/a, doi:10.1002/2015JC010889,  
23 2015.
- 24 Ohde, T., Fiedler, B. and Körtzinger, A.: Spatio-temporal distribution and transport of  
25 particulate matter in the eastern tropical North Atlantic observed by Argo floats, *Deep Sea*  
26 *Res. Part I Oceanogr. Res. Pap.*, 102, 26–42, doi:10.1016/j.dsr.2015.04.007, 2015.
- 27 Pastor, M. V, Pelegrí, J. L., Hernández-Guerra, A., Font, J., Salat, J. and Emelianov, M.:  
28 Water and nutrient fluxes off Northwest Africa, *Cont. Shelf Res.*, 28(7), 915–936 [online]  
29 Available from: <http://www.sciencedirect.com/science/article/pii/S0278434308000265>, 2008.
- 30 Picheral, M., Guidi, L., Stemmann, L., Karl, D. M., Iddaoud, G. and Gorsky, G.: The





- 1 Underwater Vision Profiler 5: An advanced instrument for high spatial resolution studies of  
2 particle size spectra and zooplankton, *Limnol. Oceanogr. Methods*, 8, 462–473,  
3 doi:10.4319/lom.2010.8.462, 2010.
- 4 Redfield, A. C., Ketchum, B. H. and Richards, F. A.: The influence of organisms on the  
5 composition of seawater, in *The Sea*. Interscience, edited by M. N. Hill, pp. 26–77., 1963.
- 6 Roemmich, D., Johnson, G., Riser, S., Davis, R. and Gilson, J.: The Argo Program: observing  
7 the global ocean with profiling floats, *Oceanography*, 22(2), 34–43 [online] Available from:  
8 <http://darchive.mblwhoilibrary.org:8080/handle/1912/2980> (Accessed 15 July 2010), 2009.
- 9 Rossi, V., López, C., Hernández-García, E., Sudre, J., Garçon, V. and Morel, Y.: Surface  
10 mixing and biological activity in the four Eastern Boundary Upwelling Systems, *Nonlinear*  
11 *Process. Geophys.*, 16(4), 557–568, doi:10.5194/npg-16-557-2009, 2009.
- 12 Schütte, F., Brandt, P. and Karstensen, J.: Occurrence and characteristics of mesoscale eddies  
13 in the tropical northeast Atlantic Ocean, *Ocean Sci. Discuss.*, 12(6), 3043–3097,  
14 doi:10.5194/osd-12-3043-2015, 2015.
- 15 Schütte, F., Karstensen, J., Krahnemann, G., Hauss, H., Fiedler, B., Brandt, P., Visbeck, M. and  
16 Körtzinger, A.: Characterization of “dead-zone ” eddies in the tropical Northeast Atlantic  
17 Ocean, *Biogeosciences Discuss.*, (Special Issue), in prep.
- 18 Shih, Y.-Y., Hung, C.-C., Gong, G.-C., Chung, W.-C., Wang, Y.-H., Lee, I.-H., Chen, K.-S.  
19 and Ho, C.-Y.: Enhanced Particulate Organic Carbon Export at Eddy Edges in the  
20 Oligotrophic Western North Pacific Ocean, *PLoS One*, 10(7), e0131538 [online] Available  
21 from: <http://dx.doi.org/10.1371/journal.pone.0131538>, 2015.
- 22 Stramma, L., Hüttl, S. and Schafstall, J.: Water masses and currents in the upper tropical  
23 northeast Atlantic off northwest Africa, *J. Geophys. Res.*, 110(C12), C12006,  
24 doi:10.1029/2005JC002939, 2005.
- 25 Stramma, L., Johnson, G. C., Sprintall, J. and Mohrholz, V.: Expanding Oxygen-Minimum  
26 Zones in the Tropical Oceans, *Science* (80-. ), 320(5876), 655–658 [online] Available from:  
27 <http://www.sciencemag.org/content/320/5876/655.abstract>, 2008a.
- 28 Stramma, L., Brandt, P., Schafstall, J., Schott, F., Fischer, J. and Körtzinger, A.: Oxygen  
29 minimum zone in the North Atlantic south and east of the Cape Verde Islands, *J. Geophys.*  
30 *Res.*, 113(C4), 1–15, doi:10.1029/2007JC004369, 2008b.



- 1 Stramma, L., Visbeck, M., Brandt, P., Tanhua, T. and Wallace, D.: Deoxygenation in the  
2 oxygen minimum zone of the eastern tropical North Atlantic, *Geophys. Res. Lett.*, 36(20),  
3 L20607, doi:10.1029/2009GL039593, 2009.
- 4 Stramma, L., Prince, E. D., Schmidtko, S., Luo, J., Hoolihan, J. P., Visbeck, M., Wallace, D.  
5 W. R., Brandt, P. and Kortzinger, A.: Expansion of oxygen minimum zones may reduce  
6 available habitat for tropical pelagic fishes, *Nat. Clim. Chang.*, 2(1), 33–37 [online] Available  
7 from: <http://dx.doi.org/10.1038/nclimate1304>, 2012.
- 8 Stramma, L., Bange, H. W., Czeschel, R., Lorenzo, A. and Frank, M.: On the role of  
9 mesoscale eddies for the biological productivity and biogeochemistry in the eastern tropical  
10 Pacific Ocean off Peru, *Biogeosciences*, 10(11), 7293–7306, doi:10.5194/bg-10-7293-2013,  
11 2013.
- 12 Sugimura, Y. and Suzuki, Y.: A high-temperature catalytic oxidation method for the  
13 determination of non-volatile dissolved organic carbon in seawater by direct injection of a  
14 liquid sample, *Mar. Chem.*, 24(2), 105–131, doi:10.1016/0304-4203(88)90043-6, 1988.
- 15 Tomczak, M.: An analysis of mixing in the frontal zone of South and North Atlantic Central  
16 Water off North-West Africa, *Prog. Oceanogr.*, 10(3), 173–192, doi:10.1016/0079-  
17 6611(81)90011-2, 1981.
- 18 Wolf-Gladrow, D. A., Zeebe, R. E., Klaas, C., Kortzinger, A. and Dickson, A. G.: Total  
19 alkalinity: The explicit conservative expression and its application to biogeochemical  
20 processes, *Mar. Chem.*, 106, 287–300 [online] Available from:  
21 <http://oceanrep.geomar.de/11417/>, 2007.
- 22  
23



1 Table 1 Overview of detected concentration anomalies ( $\Delta_{\text{total}}$ ) within the ACME core  
 2 during the two surveys referenced against prevailing conditions at the shelf. Rate estimates  
 3 are based on the lifetime of the ACME derived from satellite sea level anomaly data (ISL: 163  
 4 days, M105: 173 days). Values for the average shelf profile are given in order to illustrate  
 5 local variability at the corresponding isopycnal ( $=26.35 \text{ kg m}^{-3} - 1000$ ).

	ISL		M105		Shelf	
	05 – 07 March 14		17-18 March 14		June / July	
	$\Delta_{\text{total}}$ (unit)	Rate (unit d <sup>-1</sup> )	$\Delta_{\text{total}}$ (unit)	Rate (unit d <sup>-1</sup> )	Mean (unit)	SD (unit)
Salinity (psu)	-0.082	< 0.004	-0.054	< 0.002	35.588	0.124
Temp. (°C)	-0.280	-0.002	-0.184	-0.001	15.353	0.415
O <sub>2</sub> (μmol kg <sup>-1</sup> )	-35.56	-0.22	-44.42	-0.26	48.95	8.88
NO <sub>3</sub> <sup>-</sup> (μmol kg <sup>-1</sup> )	3.48	0.02	5.02	0.03	25.77	1.62
NO <sub>2</sub> <sup>-</sup> (μmol kg <sup>-1</sup> )	-0.08	< -0.001	< -0.01	< 0.001	0.09	0.11
PO <sub>4</sub> <sup>3-</sup> (μmol kg <sup>-1</sup> )	0.29	< 0.01	0.34	< 0.01	1.60	0.14
SIO <sub>2</sub> (μmol kg <sup>-1</sup> )	2.05	0.01	2.52	0.01	6.73	1.27
DIC (μmol kg <sup>-1</sup> )	35.1	0.2	39.8	0.2	2218.7	1.4
TA (μmol kg <sup>-1</sup> )	-10.8	< 0.1	-12.3	< 0.1	2331.5	7.5
pCO <sub>2</sub> μatm	268.68	1.65	332.67	1.92	827.93	28.15
pH	-0.12	< -0.01	-0.14	< -0.01	7.77	0.01
Ω <sub>Ar</sub>	-0.38	< -0.01	-0.43	< -0.01	1.48	0.08

6

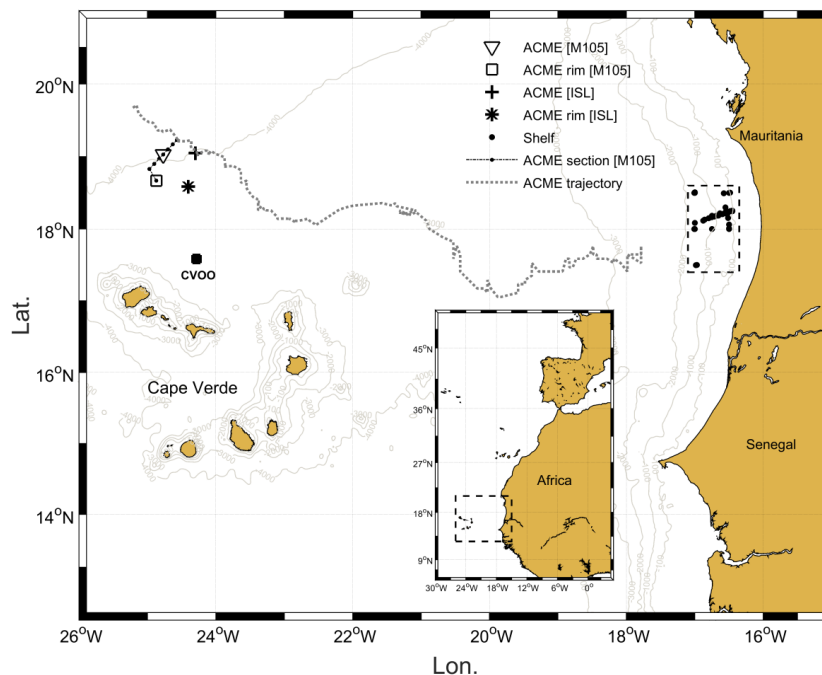
7



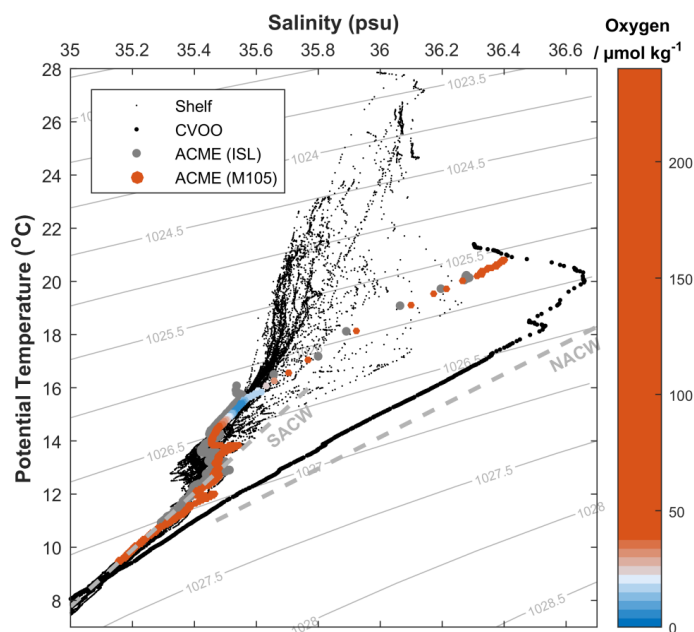
1 Table 2 Comparison of  $F_{100}$  values from the literature representing different ocean  
 2 regions with the results of this study.

Region	$F_{100}$ (g C m <sup>-2</sup> d <sup>-1</sup> )	Method	Reference
ETNA (ACME)	0.19 – 0.23	aOUR	this study
ETNA (CE)	0.24	aOUR	this study (data from Karstensen et al. 2015)
West Pacific (CE)	0.13 – 0.19	Trap	Shih et al. 2015
ETNA (open ocean)	0.11	aOUR	Karstensen et al. 2008
N. Atl. (bloom)	0.29	Thorium, Trap	Berelson 2001
Arab. Sea	0.03 – 0.11	Thorium	Lee et al. 1998
N. Pac. Gyre (HOT)	0.03	Trap	Buesseler et al. 2007
N. Pac. (K2)	0.03 – 0.08	Trap	Buesseler et al. 2007
N. Atl. (Gyre)	0.02	Trap	Marsay et al. 2015
N. Atl. (Gyre)	0.15	aOUR	Jenkins 1982
NE Pac.	0.05	Trap	Martin et al. 1987b

3

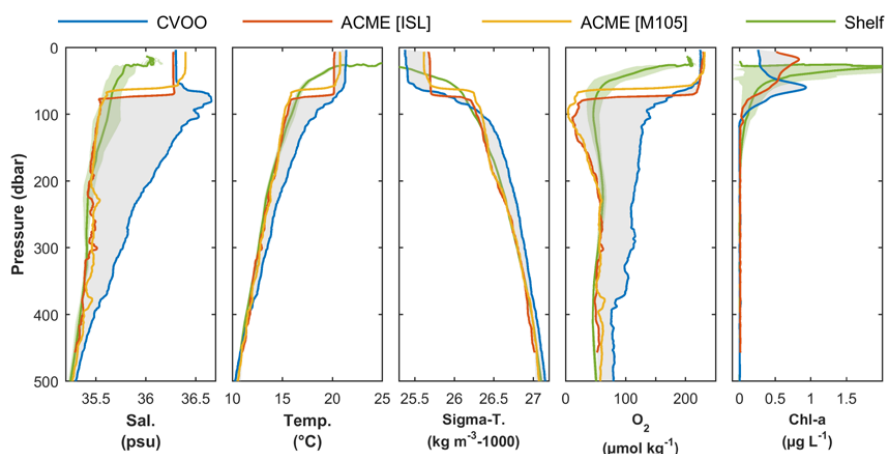


1  
2 Figure 1 Map of the study area between the Mauritanian coast and the Cape Verde  
3 Archipelago. The ACME trajectory (dotted line) is based on satellite sea level anomaly data  
4 and starts off the Mauritanian shelf edge in Sept. 2013. In March 2014, the ACME was  
5 surveyed twice north of Cape Verde with two different research vessels: RV Islândia (ISL)  
6 and RV Meteor (M105). The area marked on the Mauritanian shelf (dashed line) represents  
7 the area where the ACME was most likely created and which serves as a reference for initial  
8 conditions within the eddy.



1  
2  
3  
4  
5  
6  
7

Figure 2 Temperature-Salinity (TS) diagram containing data from both eddy surveys (colored and gray dots), the nearby CVOO station (large black dots) and accumulated CTD hydrocast data from multiple surveys on the shelf (small black dots). Dashed gray lines indicate typical NACW and SACW water mass signatures after Tomczak (1981).

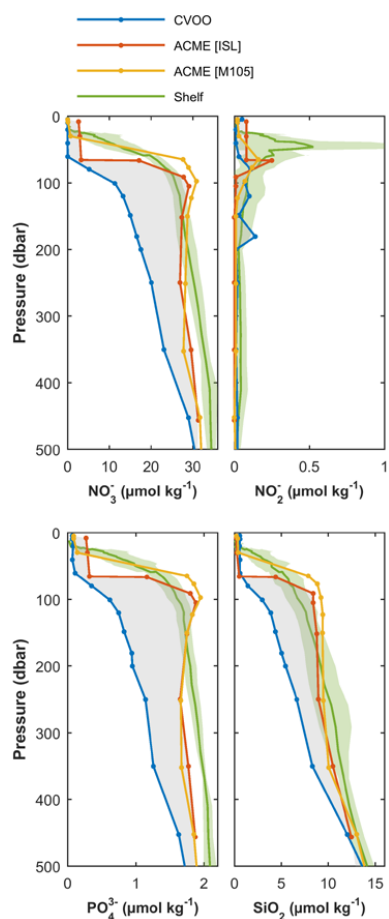


1  
2 Figure 3 Vertical profiles for all parameters measured from sensors mounted on CTD rosette  
3 systems. Data from the nearby CVOO station (blue) represent local background conditions,  
4 the gray area emphasizes the local anomaly against the background introduced by the ACME  
5 (yellow and red) and the green curve represents mean initial conditions of the ACME at the  
6 shelf (light green indicates standard deviation of the mean profile). Note that not all surveys  
7 were carried out with the same sensor package.

8



1



2

3 Figure 4 Discrete bottle data for nutrients from the different ACME surveys. The grey  
4 shading illustrates the anomaly of the ACME (ISL) with respect to the regional background  
5 situation (CVOO).

6

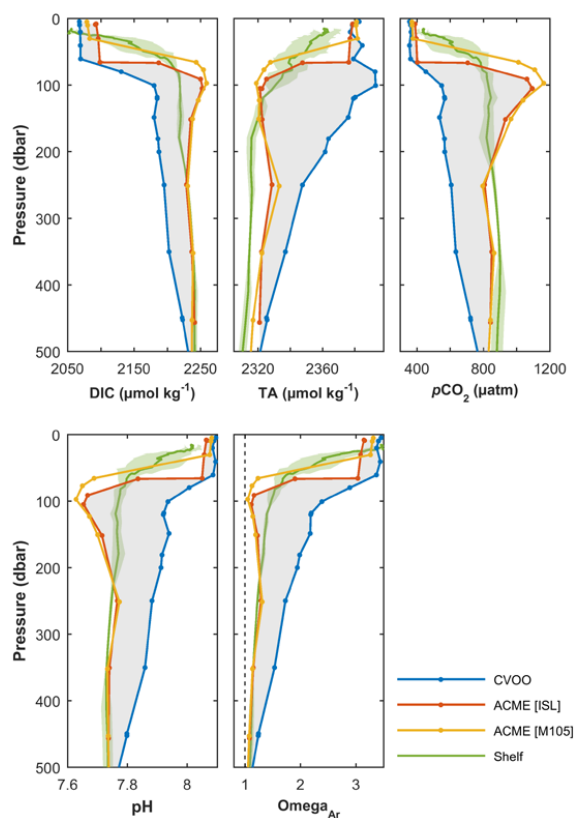
7

8

9

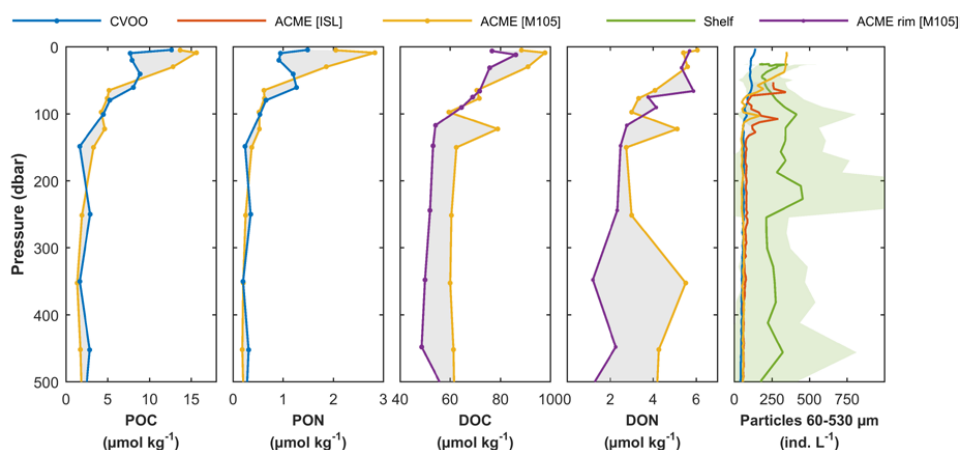
10





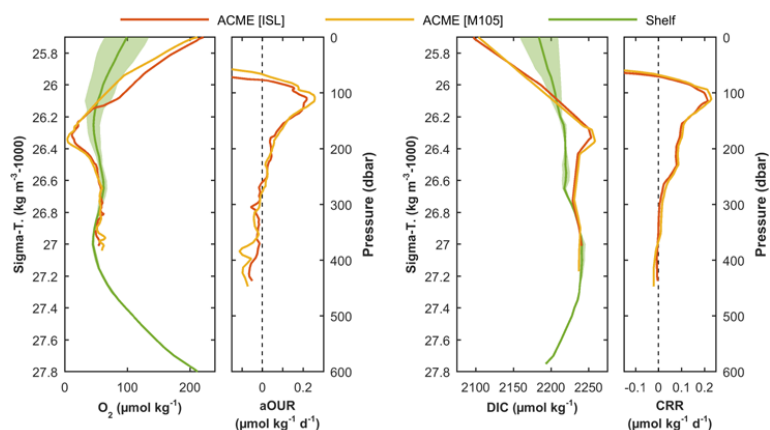
1  
2  
3  
4  
5  
6

Figure 5 Discrete bottle data for DIC and TA and calculated parameters of the carbonate system (pH,  $p\text{CO}_2$  and  $\Omega_{\text{Ar}}$ ) from the different ACME surveys. The grey shading illustrates the anomaly of the ACME (ISL) with respect to the regional background situation (CVOO).



1  
 2 Figure 6 Vertical Distribution of particulate and dissolved organic matter (first 4 panels)  
 3 based on discrete samples and particle density (60 – 530 µm) derived from high resolution  
 4 UVP data (right panel). Note that no data at CVOO exist for DOC and DON, hence data from  
 5 the eddy rim station is shown.

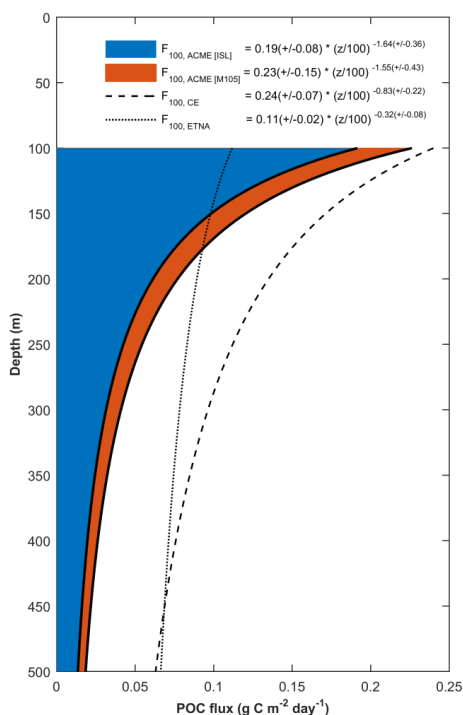
6



7  
 8 Figure 7 Estimated biogeochemical rates within the ACME as derived along isopycnals  
 9 between the shelf (green) and the ACME at the time of the two surveys (red, yellow). This  
 10 approach is illustrated for oxygen and DIC profile data (large panels). Corresponding aOUR  
 11 and CRR are peaking in the core of the ACME (small panels). Note that the matching  
 12 between shelf and ACME data was made in density space whereas the resulting rates are  
 13 plotted in depth space.



1



2

3 Figure 8 Derived downward POC fluxes based on a model after Martin et al. (1987b) for  
4 the two ACME surveys (blue and red), a cyclonic eddy sampled by an Argo float (CE, dashed  
5 line; Karstensen et al., 2015) and the general ETNA (Karstensen et al., 2008). Flux estimates  
6 for the two ACME surveys are based on CRRs estimated from DIC sample data. For the CE,  
7 aOURs derived from oxygen measurements on an Argo float were converted to CRRs by  
8 applying a stoichiometric  $-O_2:C$  ratio of 1.34 (Körtzinger et al., 2001b). Background POC  
9 flux in the ETNA was estimated from large scale thermocline aOURs derived from transient  
10 tracer data and AOU (Karstensen et al., 2008) followed by a stoichiometric conversion as  
11 described above.